Journal of Materials Chemistry A

Efficient and thermally stable all-polymer solar cells based on a fluorinated wide bandgap polymer donor with high crystallinity

Journal:	*Journal of Materials Chemistry A*
Manuscript ID	TA-ART-06-2018-005376.R1
Article Type:	Paper
Date Submitted by the Author:	07-Jul-2018

Complete List of Authors:	Su, Wenyan; Xiangtan University Meng, Yuan; Soochow University Guo, Xia; Soochow University, Laboratory of Advanced Optoelectronic Materials, College of Chemistry, Chemical Engineering and Materials Science Fan, Qunping; Soochow University, Zhang, Ming ; Shanghai Jiao Tong University Jiang, Yufeng ; Polymer Science and Engineering Department University of Massachusetts Amherst, Xu, Zhuo; Soochow University, College of Chemistry, Chemical Engineering and Materials Science Dai, Yu; Soochow University Xie, Beichen ; Soochow University Liu, Feng; Shanghai Jiao Tong University Zhang, Maojie; Soochow University, Laboratory of Advanced Optoelectronic Materials, College of Chemistry, Chemical Engineering and Materials Science Russell, Thomas; University of Massachusetts, Polymer Science and Engineering Department Li, Yongfang; Chinese Academy of Sciences, Institute of Chemistry

Efficient and thermally stable all-polymer solar cells based on a fluorinated wide bandgap polymer donor with high crystallinity

Wenyan Su,[‡a] Yuan Meng,[‡a] Xia Guo,*[a] Qunping Fan,[a] Ming Zhang,[b] Yufeng Jiang,[c] Zhuo Xu,[a] Yu Dai,[a] Beichen Xie,[a] Feng Liu,*[b] Maojie Zhang,*[a] Thomas P. Russell[c] and Yongfang Li[ad]

[a] Laboratory of Advanced Optoelectronic Materials, College of Chemistry, Chemical Engineering and Materials Science, Soochow University, Suzhou 215123, China.

*E-mail: mjzhang@suda.edu.cn; guoxia@suda.edu.cn

[b] Department of Physics and Astronomy, Shanghai Jiaotong University, Shanghai, China

*E-mail: fengliu82@sjtu.edu.cn

[c] Materials Sciences Division, Lawrence Berkeley National Laboratory, Berkeley, CA, USA

[d] Beijing National Laboratory for Molecular Sciences, CAS Key Laboratory of Organic Solids, Institute of Chemistry, Chinese Academy of Sciences, Beijing 100190, China.

[‡] These authors contributed equally to this work.

Abstract: All-polymer solar cells (all-PSCs) based on *n*-type polymer as acceptor and *p*-type polymer as donor materials have attracted great attention due to their excellent device stability. However, a systematic study of thermal stability for all-PSCs has not been reported to date. Herein, we developed a high efficiency and thermally stable all-PSCs based on a fluorinated wide bandgap polymer donor (PFBZ) and a narrow bandgap polymer acceptor (N2200). The PFBZ:N2200 pair shows complementary absorption spectra, matched energy levels and good blend morphology. As a result, the PFBZ:N2200-based devices under thermal annealing at 150 ˚C for 15 min achieved a high power coversion efficiency (PCE) of 8.1% with high open-circuit voltage of 0.90 V, short-circuit current density of 13.5 mA cm^{-2}, fill factor of 67.0% as well as low energy loss of 0.56 eV. The efficiency of 8.1% is one of the highest values

reported for the additive-free all-PSCs. When the thermal annealing time is extended to 180 min or the temperature is increased to 250 ˚C, the all-PSCs still retained a high PCE of over 7%. The results indicate that the PFBZ:N2200-based all-PSCs with high efficiency and excellent thermal stability are promising candidates for the practical applications of OSCs.

Keywords: Thermal stability; fluorinated wide bandgap polymer; power conversion efficiency; all-polymer solar cells

1. Introduction

Polymer solar cells (PSCs), containing the bulk heterojunction active layers consisting of a polymer donor and a small molecule (SM) acceptor such as fullerene derivatives[1-5] or *n*-type organic semiconductors (*n*-OSs),[6-10] have attrated great attention due to their advantages such as large-scale manufacturing and compatibility with semitransparency and flexibility. So far, the power conversion efficiencies (PCEs) of the PSCs based on fullerene derivative or *n*-OSs as acceptors have reached 11%[11] and 13%[12], respectively. However, the above type PSCs usually show poor thermal stability, which may be due to the self-aggregation of SM-acceptors in high temperature atomosphere, resulting in lower exciton separation efficiency, reduced charge extraction abilities, and increased charge recombination in devices. Compared to the extensively studied polymer:SM-acceptor devices, all-PSCs based on polymers donor and acceptor have unique the morphological stability of active layer to external factors, especially mechanical stress and thermal, for practic applications as flexible devices in the future.[13-17] Among them, the naphthalene diimide and perylene diimide derivatives-containing n-type conjugated polymer acceptors have been well studied for the application in the all-PSCs.[18-22] So far, the all-PSCs have achieved high PCEs of 8-10% benefited from the development of new polymers donor and acceptor materials and the optimization of the devices.[23-26] For exmaple, Zhang *et al.* reported an excellent polymer acceptor namely PZ1

with narrow bandgap (NBG) and high absorption coefficient, suitable energy levels, high electron mobility and electron affinity.[23a] By matching a wide bandgap (WBG) polymer donor with a complementary absorption spectrum to PZ1, the all-PSCs show a high PCE of 9.19% with a high short-circuit current density (J_{sc}) of 16.05 mA cm^{-2}. Very recently, Huang *et al.* synthesized a WBG polymer named PTzBI-Si with siloxane-terminated side-chain as donor for photovoltaic applications, and achieved a PCE of more than 10% in all-PSCs for the first time.[24a] Although their have many unique advantages and have made great progress, the systematic study of thermal stability of the all-PSCs is still rarely reported.

So far, the most studied D/A pair is PTB7-Th:N2200 in all-PSCs and has already achieved PCEs of more than 6%.[27-29] However, the PTB7-Th:N2200 pair has many inherent defects, such as the overlapping absorption spectra, the mismatched energy levels and the poor phase separation result in small J_{sc}, open-circuit voltage (V_{oc}) and fill factor (FF) respectively, which seriously restricts the further promotion of its efficiency. Our previous work has shown that the efficiency of the PTB7-Th:N2200-based all-PSCs can be effectively improved from 5.9% to 7.2% by introducing a small amount of WBG polymer PBDD-ff4T with strong crystallinity to induce phase separation of active layer for optimize the blend morphologies.[30a] However, due to a small amount of third components can not effectively optimize the optical absorption and energy level of active layer, the V_{oc} and J_{sc} values of all-PSCs are not maximized. Therefore, an effective and challenging strategy to promote efficiency of the N2200-based devices is to develop the binary all-PSCs by matching a WBG polymer donor with strong crystallinity and suitable energy levels for N2200.

Recently, researchers reported a series of WBG polymer donors[7a,31] and narrow bandgap SM-acceptors[32-34] with strong crystallinity based on benzotriazole (BTz) as acceptor unit. Among them, the fluorinated WBG polymer donor named PFBZ[31a] with strong crystallinity,

high extinction coefficient and suitable energy levels was recently reported by our group. The PSCs based on the blend PFBZ:ITIC displayed a high PCE of 10.4%.

Herein, we developed a high efficiency and thermally stable binary all-PSCs based on a D/A pair of PFBZ:N2200. The PFBZ:N2200 pair shows complementary absorption spectra, matched energy levels and different crystallinity. As expected, the PFBZ:N2200-based all-PSCs processed with thermal annealing at 150 ˚C for 15 min achieved a high efficiency PCE of 8.1% with high V_{oc} of 0.90 V, J_{sc} of 13.5 mA cm^{-2} and FF of 67.0%. The efficiency of 8.1% is one of the highest values reported for the additive-free all-PSCs. Notably, the optimal all-PSCs also showed a low energy loss (E_{loss}, is defined as E_g^{opt}-eV_{oc}) of *ca.* 0.56 eV due to the small optical bandgap (E_g^{opt}, *ca.* 1.46 eV) of the N2200 film, which is less than the empirical threshold of 0.6 eV. When the thermal annealing time is extended to 180 min at 150 ˚C, the all-PSCs still retained a high PCE of 7.1%. Moreover, after increasing the thermal annealing temperature to 250 ˚C for 15 min, the all-PSCs also retained a PCE of more than 7%. Further, in order to have an insight into the thermal stability of devices, the effect of different thermal annealing temperature and annealing time on the morphology and photoluminescence (PL) properties of the active layer, as well as the exciton separation, charge extraction and recombination of all-PSCs also were studied. Our results indicate that the all-PSCs based on PFBZ:N2200 have high efficiency and excellent thermal stability, and are promising candidates for the practical applications of OSCs.

2. Results and Discussion

The normalized UV-vis absorption spectra of the polymer films and the corresponding blend film are shown in Fig. 1b. The fluorinate polymer PFBZ film possesses strong absorption at a wavelength range of *ca.* 450-630 nm, which complements the absorption spectrum of NBG polymer N2200 film with two absorption bands in the short wavelength region of *ca.* 300-450 nm and the long wavelength region of *ca.* 630-850 nm. As a result, the

PFBZ:N2200 blend film shows a fully absorbed spectrum from *ca.* 300-850 nm, which is beneficial to the related all-PSCs to capture more photons. It is worth noting that in the blend film, the absorption spectrum belonging to PFBZ is well preserved in comparison with the pure PFBZ film, which implies that PFBZ can crystallize alone and keep the original crystallinity in the blend film, thus promoting the phase separation.[31a,35] Moreover, PFBZ shows a stronger absorption compared to N2200 in the blend film, which is consistent with the higher absorption coefficient and crystallinity of PFBZ.[30,31a] The molecular energy levels of polymers PFBZ and N2200 was summarized in Fig. 1c. The PFBZ:N2200 pair shows large ΔE_{HOMO} ($HOMO_{donor}$ - $HOMO_{acceptor}$) and ΔE_{LUMO} ($LUMO_{donor}$ - $LUMO_{acceptor}$) values of 0.37 and 0.70 eV respectively, which provides a strong driving force for the exciton separation at the PFBZ:N2200 interfaces. Moreover, the large gap (*ca.* 1.24 eV) between $HOMO_{donor}$ and $LUMO_{acceptor}$ is beneficial to the all-PSCs to gain high V_{oc}.

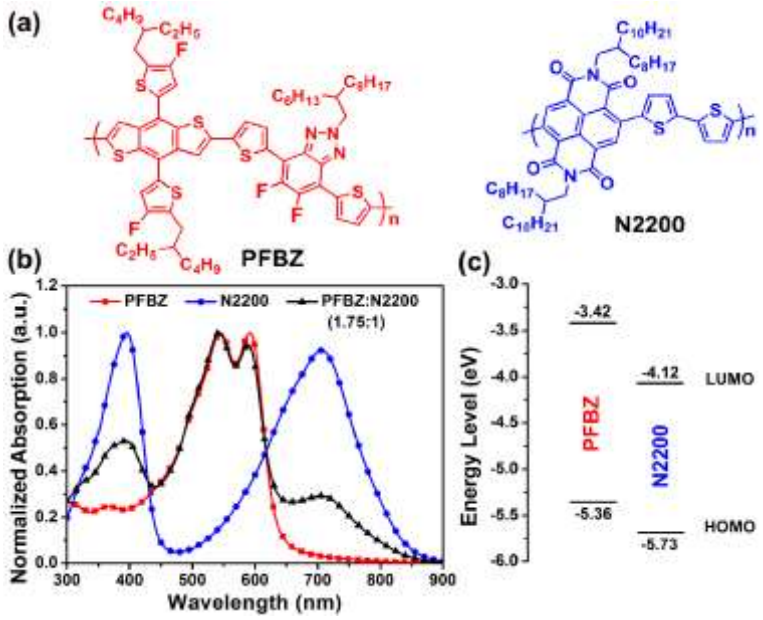

Fig. 1. (a) Molecular structures of polymers PFBZ and N2200. (b) Absorption spectra of polymers PFBZ and N2200 and the corresponding PFBZ:N2200 blend films. (c) Molecular energy level diagrams of polymers PFBZ and N2200.

The all-PSCs with a device structure of glass/ITO/PEDOT:PSS/PFBZ:N2200/PDINO/Al were fabricated, and the related preparation processes are summarized in Fig. S1 and Table S1 of Supporting Information (SI). The chlorobenzene solution of blending PFBZ and N2200 (9 mg mL^{-1}) was heated to 100 ˚C for 20 h and then cooled to 65 ˚C for 15 min before being used. For the weight ratios of PFBZ:N2200 from 1.5:1 to 2:1, the all-PSCs show PCEs over 5.5% with high V_{oc} of 0.89-0.90 V, and an optimal PCE of 6.1% was obtained at a weight ratio of 1.75:1. And then, the blend morphology of PFBZ:N2200 (1.75:1) was optimized by thermal annealing treatments. After the active layer processed by annealing at 150 ^{o}C for 15 min, the all-PSCs exhibited a significantly increased J_{sc} from 11.9 to 13.5 mA cm^{-2} and a remarkably improved FF from 56.7% to 67.0% simultaneously, while the V_{oc} was almost constant 0.90 V (see Fig. 2a and Table 1). Moreover, the optimal all-PSCs also showed a low E_{loss} of *ca.* 0.56 eV, which is less than the empirical threshold of 0.6 eV. As a result, the all-PSCs gained an optimal efficiency of 8.1%, which is one of the highest values reported for the additive-free all-PSCs.

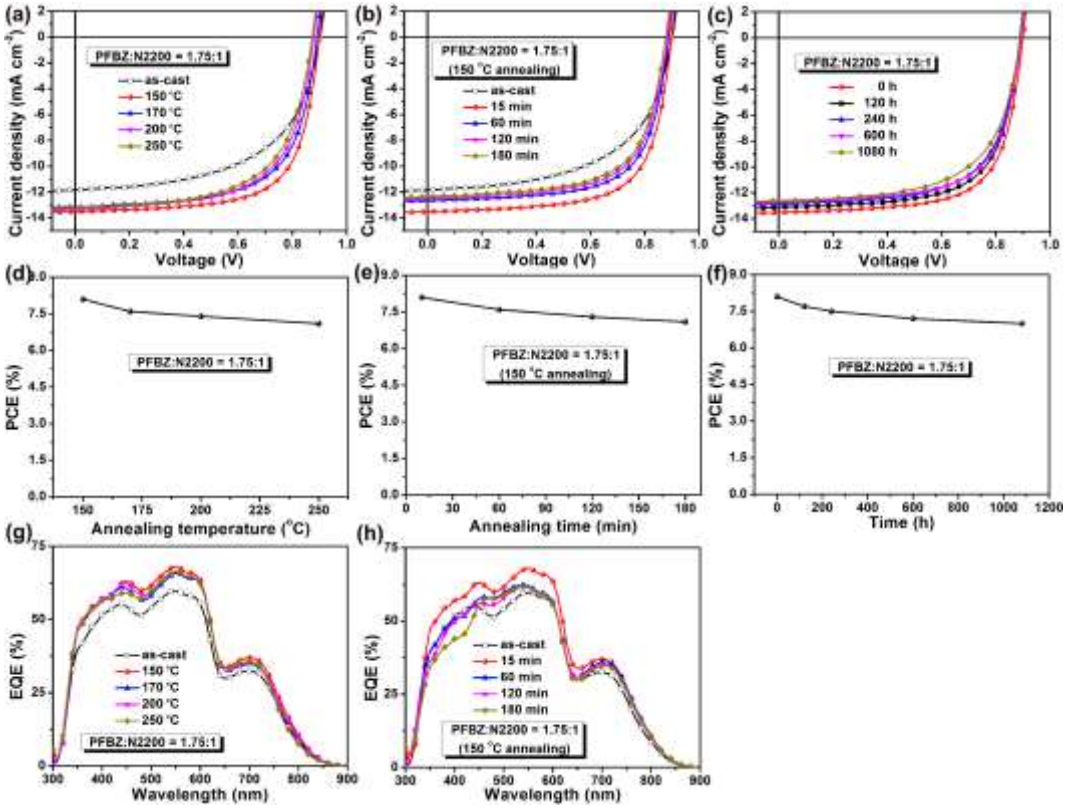

Fig. 2. (a) The *J*-*V* and (d) EQE curves, and (g) the corresponding PCEs versus annealing temperatures for 15 min of the all-PSCs. (b) The *J*-*V* and (e) EQE curves, and (h) the corresponding PCEs versus annealing times under a annealing temperature of 150 ˚C of the all-PSCs. (c) The *J*-*V* and f) the corresponding PCEs versus storage times of the all-PSCs in the N_2-filled glovebox.

Table 1. Photovoltaic data of the PFBZ:N2200-based PSCs under AM 1.5G illumination (100 mW cm^{-2}).

	V_{oc} [V]	J_{sc}[a] [mA cm^{-2}]	FF [%]	PCE[b] [%]
As-cast	0.90	11.9 (11.5)	56.7	6.1 (5.9)
150 ˚C for 15 min	0.90	13.5 (13.1)	67.0	8.1 (7.8)
170 ˚C for 15 min	0.89	13.2 (12.6)	64.7	7.6 (7.3)
200 ˚C for 15 min	0.88	13.3 (12.8)	63.3	7.4 (7.1)
250 ˚C for 15 min	0.87	13.2 (12.5)	61.6	7.1 (6.7)
150 ˚C for 60 min	0.89	12.7 (12.2)	66.8	7.6 (7.2)
150 ˚C for 120 min	0.88	12.5 (11.9)	66.1	7.3 (6.9)
150 ˚C for 180 min	0.88	12.4 (11.8)	65.4	7.1 (6.6)
25 ˚C for 1080 h	0.89	12.6	62.2	7.0 (6.4)

[a]The integral J_{sc} in parentheses from the EQE curves. [b]The average PCEs in parentheses from 10 devices.

The thermal stabilities of the PFBZ:N2200-based all-PSCs were also studied by probing the photovoltaic performance of the devices with different annealing temperatures and annealing times. As shown in Fig. 2a, with the thermal annealing temperature continues to increase from 150 ˚C to an ultra high 250 ˚C for 15 min, the all-PSCs show gradually but only slightly decreased V_{oc} and J_{sc}. As a result, the high temperature annealed all-PSCs achieved a high PCE of 7.1% (see Fig. 2d). Moreover, as the thermal annealing time is extended to 180 min at 150 ˚C, the device efficiency still remains 87.7% and has a PCE of more than 7%, as shown in

Fig. 2b,e. Detailed photovoltaic data are summarized in Table 1. Further, the all-PSC devices also show excellent storage stability, as shown in Fig. 2c,f. After 1080 h of storage in the glovebox filled with N_2, the all-PSCs still achieve an efficiency of *ca.* 7.0% with a high PCE preservation ratio of *ca.* 86.4%. Detailed photovoltaic data are summarized in Table S2 of SI. The above results indicate that the PFBZ:N2200-based all-PSCs have excellent thermal stabilities and storage stability.

Moreover, the PSCs with different active layer thicknesses of 90~200 nm were fabricated to probe the effect of active layer thickness on the device performance (see Fig. S2 and Table S3 in SI). With increasing active layer thicknesses from *ca.* 90 nm to 200 nm, the PSCs show almost unchanged V_{oc}, small fluctuations of J_{sc} and decreased FF. Notably, when the active layer thickness is up to 200 nm, the all-PSCs still achieve a PCE of more than 6%, which is crucial for the practical mass production of PSCs.

To confirm the J_{sc} of all-PSCs, the external quantum efficiencies (EQE) were measured. As shown in Fig. 2g, with the increase of thermal annealing temperature from 150 ˚C to 250 ˚C for 15 min, the EQE response spectra of the devices have not changed obviously regardless of their shape or respnse value. As shown in Fig. 2h, with the thermal annealing time from 60 min to 180 min at 150 ˚C, the EQE response spectra of the devices also have not changed substantially, although they are obviously lower than the best all-PSCs processed with thermal annealing at 150 ˚C for 15 min. Notably, the best all-PSCs possesses a high maximum EQE value of *ca.* 68% at 550 nm, indicating that the corresponding device has efficient photon harvesting and charge collection within the cell. The integral J_{sc} values from the EQE curves are well consistent with the *J-V* tests (see Table 1).

By measuring the plots of J_{ph} versus V_{eff}, the exciton dissociation probabilities $P(E, T)$ were estimated to probe the exciton dissociation and charge extraction behaviors of the all-PSCs (Fig. 3a,c).[28,29] The parameter definitions and estimation processes are presented in detail in

SI. Under the short-circuit and maximal power output conditions, the $P(E, T)$ values were calculated to be 97.1/80.0% and 92.5/64.2% for the all-PSCs as-cast and annealed at 150 ˚C for 15 min, which implies that the annealed all-PSCs have more efficient exciton dissociation and charge extraction behaviors. With the increase of annealing temperature from 150 to 250 ˚C, the devices showed graducally but only slightly lower the $P(E, T)$ values from 97.1% to 93.2% for the short-circuit conditions and from 80.0% to 76.2% for the maximal power output conditions. With the prolongation of annealing time from 15 to 180 min, the devices also showed only slightly lower the $P(E, T)$ values from 97.1% to 95.5% for the short-circuit conditions and from 80.0% to 77.0% for the maximal power output conditions. The above results indicate that increasing the annealing temperature or prolonging the annealing time have little effect on the exciton dissociation and charge extraction behaviors of the all-PSCs devices in this case.

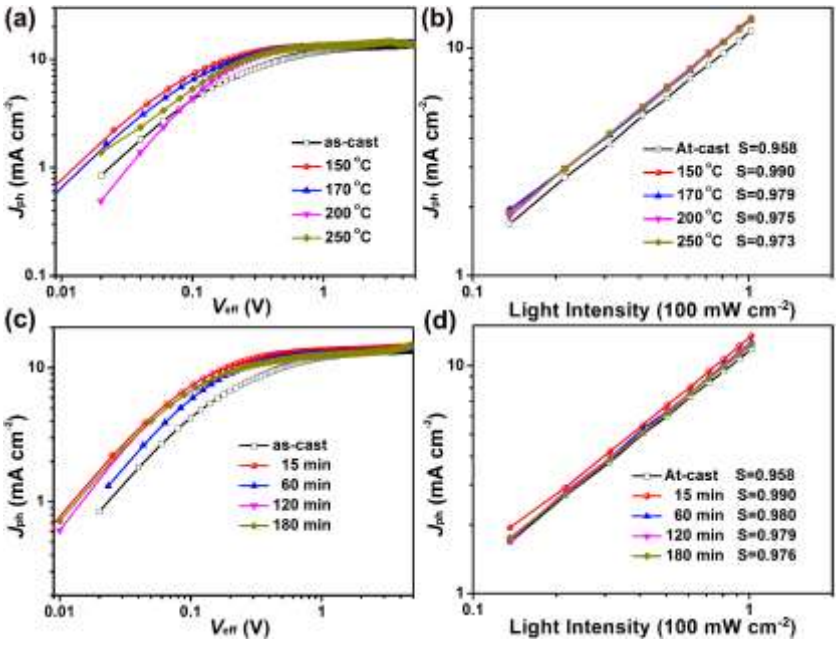

Fig. 3. The photocurrent (J_{ph}) versus effective voltage (V_{eff}) (a and c), the J_{ph} versus light intensity (P) (b and d) of the all-PSCs based on PFBZ:N2200 with different thermal annealing temperatures for 15 min and different annealing times at 150 ˚C, respectively.

Moreover, to probe the charge recombination behavior of all-PSCs, the effect of P on J_{ph} was studied (Fig. 3b,d). Generally, the P versus J_{ph} was defined as $J_{ph} \propto P^S$, and S value close to 1 if the all-PSC has weak bimolecular recombination.[12b,37] The all-PSCs processed with annealing at 150 ˚C for 15 min showed a high S value of 0.990 that is very close to 1, implying negligible bimolecular recombination and efficient charge transport in devices. By contrary, the S value of the as-cast device is 0.958, indicating the existence of bimolecular recombination to some extent. For the thermal annealed all-PSCs at 150 ˚C for 15 min, the lower bimolecular recombination agrees well with a higher FF (67.0%) compared to the as-cast all-PSCs (56.7%). This result is consistent with that the thermal annealed all-PSCs at 150 ˚C for 15 min possess the higher and more balanced hole/electron mobilities (μ_h/μ_e) of 8.72/1.62 × 10^{-4} cm^2 V^{-1} s^{-1} in comparison with the as-cast all-PSCs (6.22/0.92 × 10^{-4} cm^2 V^{-1} s^{-1}), as shown in Fig. S3. With the increase of annealing temperature from 150 to 250 ˚C or annealing time from 15 to 180 min, the devices showed gradually lower the S values from 0.990 to 0.973 or 0.976, respectively. Notably, all the annealed all-PSCs show the larger S values compared to the as-cast all-PSCs, which indicates that annealing is beneficial to the reduction of bimolecular recombination in devices of this case.

In order to more understand the high efficiency and high thermal stabilities of the PFBZ:N2200-based all-PSCs, we have measured the photoluminescence (PL) spectra of the pure PFBZ and N2200 polymer films and the corresponding PFBZ:N2200 blend films with different conditions, as shown in Fig. 4. In comparison with the PL spectra of pure PFBZ or N2200 films, the blend film annealed at 150 ˚C for 15 min showed high PL quenching efficiencies of more than 95%, while the as-cast blend film displayed low PL quenching efficiencies of less than 90%, which indicates that the all-PSCs annealed at 150 ˚C for 15 min have more efficient photo-induced charge transfer behavior between polymers PFBZ and N2200 compared to the as-cast devices. The above results are well consistent with the higher

EQE values of the annealed all-PSCs at 150 ˚C for 15 min. Notability, whether increasing thermal annealing temperatures from 150 to 250 ˚C or annealing times from 15 min to 180 min, the blend films show similar PL spectra. Moreover, the blend films possess the high PL quenching efficiencies of more than 92% and a slightly reduced tread in PL quenching efficiencies, which is consistent with the high thermal stabilities and slightly decreased PCE values (lost *ca.* 12.3%) of the all-PSCs.

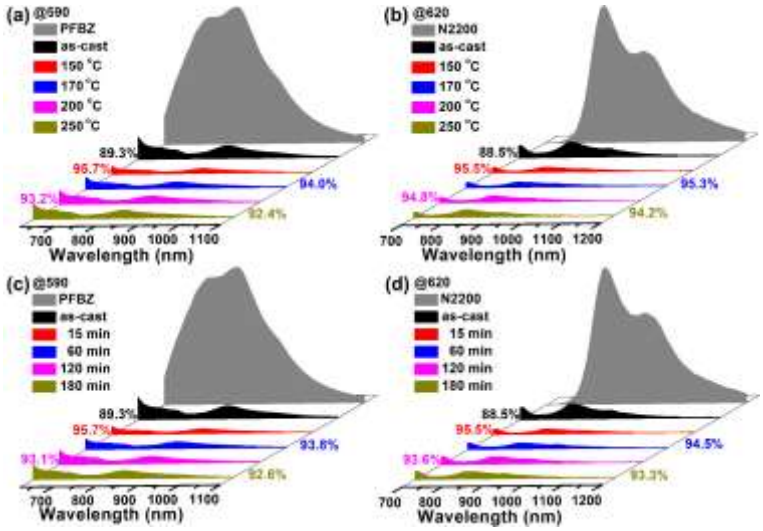

Fig. 4. The PL spectra of the pure polymers PFBZ and N2200 films and the corresponding PFBZ:N2200 blend films with different annealing temperatures for 15 min and different annealing times at 150 ˚C (excited at 590 nm for PFBZ and the related blend films, 620 nm for N2200 and the related blend films).

Grazing-incidence wide-angle X-ray diffraction (GIWAXS) was used to investigate the molecular packing in blend films. The 2D GIWAXS patterns and corresponding line-cut profiles in the in-plane and out-of-plane directions were shown in Fig. 5. For neat films, the PFBZ donor showed a dominant face-on orientation, with π-π stacking in the out-of-plane direction at 1.73 $Å^{-1}$, the crystal coherence length (CCL) of which was 2.34 nm estimated by Scherrer Equation.[38] The N2200 acceptor also showed face-on orientation, with sharp (100) reflection at 0.24 $Å^{-1}$, (200) reflection at 0.48 $Å^{-1}$ in the in-plane direction, and π-π stacking at

1.58 $Å^{-1}$ in the out-of-plane direction. CCL for (100) and π-π stacking were 9.6 nm and 1.5 nm. When donor and acceptor were mixed with each other, the crystallinity of N2200 was reduced, as evidenced by the reduced intensity of (200) peak. The π-π stacking region was composed of diffraction features from both N2200 and PFBZ that cannot be split and it was thus summarized together to estimate the overall π-π stacking feature of blend film. The board peak in the low q region was the combination of donor and acceptor (100) peaks, and it was also hard to separate them with each other. However, it could be easily seen in 2D GIWAXS image that the azimuthal spreading of (100) diffraction became narrowly distributed toward reflection horizon upon thermal annealing, especially at high temperature, which indicated that more polymer molecules were stacked in face-on fashion. For as-cast film, the CCL of N2200 (200) peak was 13.45 nm, and the CCL of π-π stacking was 1.86 nm, respectively. When 150 ˚C annealed was applied for 15 min, the blend film presented a slightly increased CCL of π-π (1.98 nm) and decreased CCL of N2200 (200) peak (12.78 nm). Extended annealing for three hours, the π-π CCL continued increasing to 2.0 nm, and N2200 (200) CCL dropping to 12.38 nm, as was shown in Fig. 5d. This trend indicated that thermal annealing at 150 ˚C reduced the structure order of N2200 but promote the crystallization of PFBZ. N2200 was known to form nano-fibrils in blend films, extended thermal annealing (3h) can thus reduce such feature, which was seen in TEM characterizations below. Thermal annealing at 250 ˚C strongly suppressed the (200) peak of N2200 and the CCL of π-π stacking was estimated to be 2.76 nm. The face-on orientation was much more prominent in this sample, as seen from the narrow distributed intensities of both overall π-π peak and (100) peak. Such results indicated that under 250 ˚C annealing, polymer chain started to reorganize with respect to substrate normal, forming better packed crystallites. Such observation was similar to previous results for N2200 and other liquid crystal conjugated polymers.[39] The amorphous halo in diffraction image (ring around 1.3 $Å^{-1}$) became less obvious in 250 ˚C annealed

sample, and thus the overall crystallinity got improved. These results revealed the fundamental importance of post-treatment details and morphology change. All-polymer blend films are a much more complicated mixture than polymer-small molecule systems, and the correlation with device performance can be more difficult. It is generally regarded that higher crystallinity can be of benefits in transporting. However, better defined packing state and CCL induced by high temperature annealing led to efficiency drop. Thus a scan of annealing time and temperature to optimize morphology will be critical. Fig. 5c showed the changes of normalized (010) peak area and device performance relationship under different annealing treatments. When annealed at 150 ˚C, 15 min could lead to slight (010) peak area increase, which then drop quickly. These results indicate that short time annealing could relive the frustration of as-cast thin film, by driving out residual solvent and reorganize related chain packing to make better π-π stacking. This step is very important in improving device performances, as seen from the quick jump in J_{sc} and FF.

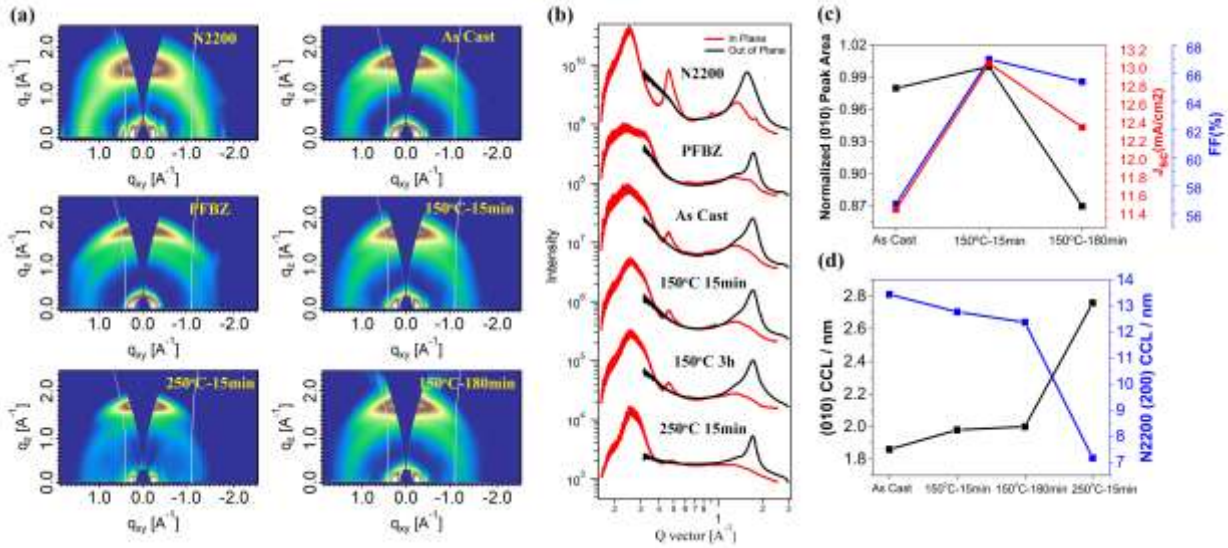

Fig. 5. (a) 2D GIWAXS diffraction pattern of thin films; (b) in-plane and out-of-plane line-cut profiles of GIWAXS results; (c) π-π stacking peak area and J_{sc} and FF correlation; (d) crystal coherence length and annealing time correlation.

The effects of different annealing temperatures and annealing times on the surface and bulk morphologies of the PFBZ:N2200 blend films were also probed. For the transmission electron microscopy (TEM) (Fig. 6), the as-cast blend film showed a large phase separation due to the strong crystallinity of the polymer donor PFBZ. After thermal annealing at 150 ˚C for 15 min, the blend film exhibited suitable phase separation, with obvious nano-networks and uniform fiber structures. It is generally believed that the suitable phase separation and fiber structure are beneficial to the J_{sc} and FF of the devices, respectively.[40] And the fibril morphology could also help to improve the charge transport of blend films.[41] With the increase of annealing temperature from 150 to 250 ˚C, the blend films still showed the suitable phase separation, although the fiber structure gradually disappears, which correlates well with the change of J_{sc} and FF in all-PSCs. On the contrary, as the increase of annealing time from 15 to 180 min at 150 ˚C, the blend films still show the fiber structures, however, the texture starts to blur. Thus extended annealing reduces the crystallinity of N2200 component, which correlate well with GIWAXS characterization.

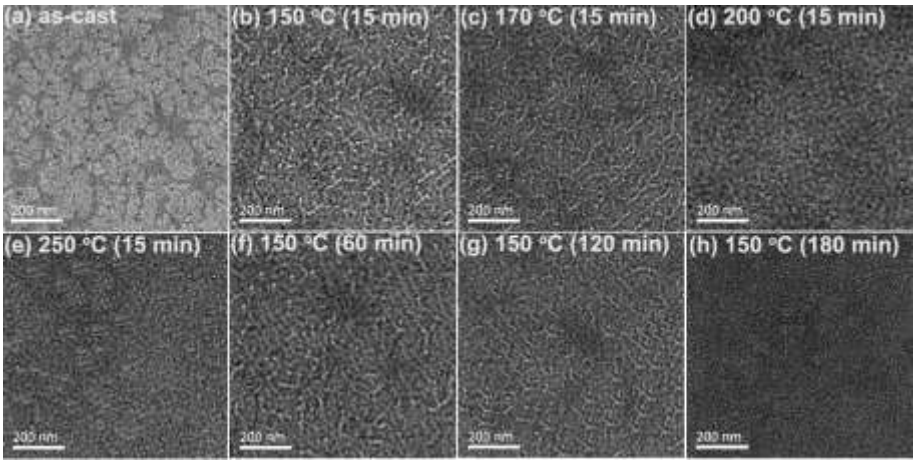

Fig. 6. TEM images of the PFBZ:N2200-based blend films with different annealing temperatures for 15 min and annealing times at 150 ˚C: (a) as-cast; (b, c, d and e) 150, 170, 200 and 250 ˚C for 15 min; (f, g, and h) 150 ˚C for 60, 120 and 180 min, respectively.

In atomic force microscopy (AFM) images (Fig. 7), with the increase of annealing temperature, the blend films showed the gradually smoothed surface and lower root-mean-square roughness (R_q) from 1.24 to 0.78 nm, which is support the disappearance of fibrils in the TEM images. When annealing at 150 ˚C, extending annealing time from 15 to 180 min does not change R_q values (1.08 ± 0.03 nm), only the as cast blend film showed a large roughness, due to large phase separated structure.

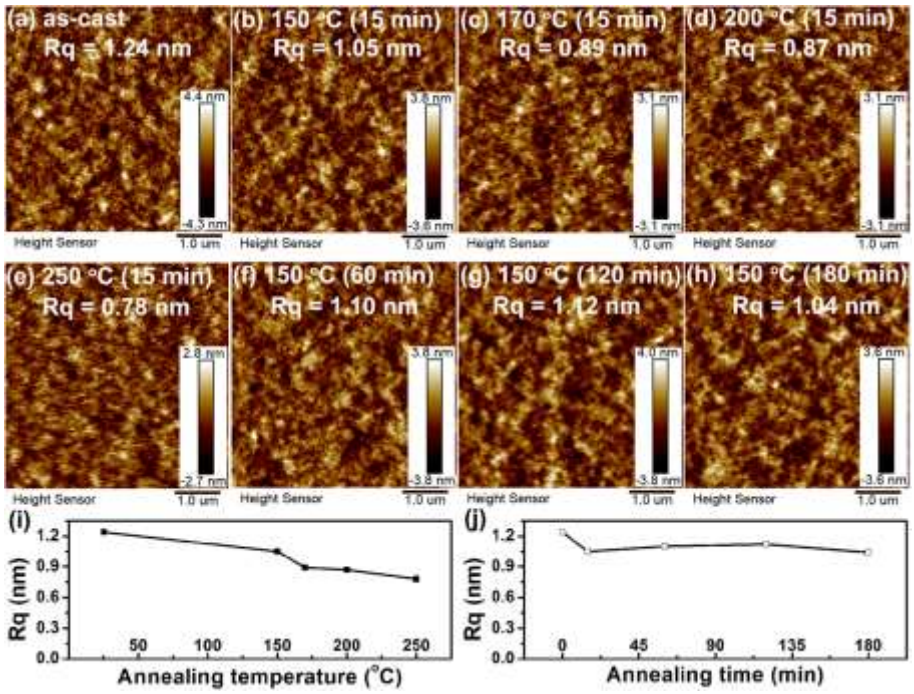

Fig. 7. AFM images of the PFBZ: N2200-based blend films with different annealing temperatures for 15 min and annealing times at 150 ˚C: (a) as-cast; (b, c, d and e) 150, 170, 200 and 250 ˚C for 15 min; (f, g and h) 150 ˚C for 60, 120 and 180 min, respectively. R_q values of the blend films with different annealing temperatures for 15 min (i) and annealing times at 150 ˚C (j).

3. Conclusions

In conclusion, a high efficiency and thermally stable all-PSC based on a PFBZ:N2200 pair with complementary absorption spectra, matched energy levels and different crystallinity. The PFBZ:N2200-based all-PSCs processed with thermal annealing at 150 ˚C for 10 min achieved

a high PCE of 8.1% with high V_{oc} of 0.90 V, J_{sc} of 13.5 mA cm^{-2}, FF of 67.0% as well as low E_{loss} of 0.56 eV. The efficiency of 8.1% is one of the highest values reported for the additive-free all-PSCs. When the annealing time is extended to 180 min at 150 ˚C, the all-PSCs still retained a high PCE of 7.1%. Moreover, after increasing the annealing temperature to 250 ˚C for 10 min, the all-PSCs have also retained a PCE of more than 7%. Notably, after 1080 h of storage in the N_2-filled glovebox, the all-PSCs also achieved a PCE of *ca.* 7.0% with a high PCE preservation ratio of *ca.* 86.4%. We also studied the effect of different annealing temperature and annealing time on the morphology and PL properties of the active layer, as well as the exciton separation, charge extraction and recombination of the all-PSCs. The results indicate that the PFBZ:N2200-based all-PSCs have high efficiency and excellent thermal stability and, are promising candidates for the practical applications of OSCs.

Acknowledgements

W.Y. Su and Y. Meng contributed equally to this work. This work was supported by National Natural Science Foundation of China (NSFC) (Nos. 51503135, 51573120 and 51773142), Jiangsu Provincial Natural Science Foundation (Grant No. BK20150332). TPR were supported by the U.S. Office of Naval Research under contract N00014-15-1-2244. Portions of this research were carried out at beamline 7.3.3 and 11.0.1.2 at the Advanced Light Source, and Molecular Foundry, Lawrence Berkeley National Laboratory, which was supported by the DOE, Office of Science, and Office of Basic Energy Sciences.

References

1. Y. Li, *Acc. Chem. Res.* 2012, **45**, 723.

2. G. Li, R. Zhu, Y. Yang, *Nat. Photonics* 2012, **6**, 153.

3. K. Kawashima, Y. Tama, H. Ohkita, I. Osaka, K. Takimiya, *Nat. Commun.* 2015, **6**, 10085.

4. a) C.-Y. Chang, L. Zuo, H.-L. Yip, Y. Li, C. Li, C.-S. Hsu, Y.-J. Cheng, H. Chen, A. K.-Y. Jen, *Adv. Funct. Mater.* 2013, **23**, 5084; b) Q. Fan, W. Su, X. Guo, X. Zhang, Z. Xu, B. Guo, L. Jiang, M. Zhang, Y. Li, *J. Mater. Chem. A* 2017, **5**, 5106; c) Z. Xu, Q. Fan, X. Meng, X. Guo, W. Su, W. Ma, M. Zhang, Y. Li, *Chem. Mater.* 2017, **29**, 4811.

5. M. Wang, H. Wang, T. Yokoyama, X. Liu, Y. Huang, Y. Zhang, T.-Q. Nguyen, S. Aramaki, G. C. Bazan, *J. Am. Chem. Soc.* 2014, **136**, 12576.

6. S. Holliday, R. S. Ashraf, A. Wadsworth, D. Baran, S. A. Yousaf, C. B. Nielsen, C. Tan, S. D. Dimitrov, Z. Shang, N. Gasparini, M. Alamoudi, F. Laquai, C. J. Brabec, A. Salleo, J. R. Durrant, I. McCulloch, *Nat. Commun.* 2016, **7**, 11585.

7. a) H. Bin, L. Gao, Z.-G. Zhang, Y. Yang, Y. Zhang, C. Zhang, S. Chen, L. Xue, C. Yang, M. Xiao, Y. Li, *Nat. Commun.* 2016, **7**, 13651; b) Q. Fan, Y. Wang, M. Zhang, B. Wu, X. Guo, Y. Jiang, W. Li, B. Guo, C. Ye, W. Su, J. Fang, X. Ou, F. Liu, Z. Wei, T. C. Sum, T. P. Russell, Y. Li, *Adv. Mater.* 2018, **30**, 1704546; c) Y. Wang, Q. Fan, X. Guo, W. Li, B. Guo, W. Su, X. Ou, M. Zhang, *J. Mater. Chem. A* 2017, **5**, 22180.

8. a) Y.-J. Hwang, H. Li, B. A. E. Courtright, S. Subramaniyan, S. A. Jenekhe, *Adv. Mater.* 2016, **28**, 124; b) D. Sun, D. Meng, Y. Cai, B. Fan, Y. Li, W. Jiang, L. Huo, Y. Sun, Z. Wang, *J. Am. Chem. Soc.* 2015, **137**, 11156.

9. Y. Lin, J. Wang, Z.-G. Zhang, H. Bai, Y. Li, D. Zhu, X. Zhan, *Adv. Mater.* 2015, **27**, 1170.

10. Y. Li, J.-D. Lin, X. Che, Y. Qu, F. Liu, L.-S. Liao, S. R. Forrest, *J. Am. Chem. Soc.* 2017, **139**, 17114.

11. J. Zhao, Y. Li, G. Yang, H. Lin, H. Ade, W. Ma, H. Yan, *Nat. Energy* 2016, **1**, 15027.

12. a) W. Zhao, S. Li, H. Yao, S. Zhang, Y. Zhang, B. Yang, J. Hou, *J. Am. Chem. Soc.* 2017, **139**, 7148; b) Q. Fan, W. Su, Y. Wang, B. Guo, Y. Jiang, X. Guo, F. Liu, P. R. Thomas,

M. J. Zhang, Y. F. Li, *Sci. China Chem.* 2018, **61**, 531; c) X. Xu, T. Yu, Z. Bi, W. Ma, Y. Li, Q. Peng, *Adv. Mater.* 2017, **30**, 1703973; d) W. Zhao, S. Zhang, Y. Zhang, S. Li, X. Liu, C. He, Z. Zheng, J. Hou, *Adv. Mater.* 2018, **30**, 1704837; e) Q. Fan, Q. Zhu, Z. Xu, W. Su, J. Chen, J. Wu, X. Guo, W. Ma, M. Zhang, Y. Li, *Nano Energy* 2018, **48**, 413.

13. a) T. Kim, J.-H. Kim, T. E. Kang, C. Lee, H. Kang, M. Shin, C. Wang, B. Ma, U. Jeong, T.-S. Kim, B. J. Kim, *Nat. Commun.* 2015, **6**, 8547; b) J. Yang, B. Xiao, K. Tajima, M. Nakano, K. Takimiya, A. Tang, E. Zhou, *Macromolecules* 2017, **50**, 3179; c) X. Wang, L. Lv, L. Li, Y. Chen, K. Zhang, H. Chen, H. Dong, J. Huang, G. Shen, Z. Yang, H. Huang, *Adv. Funct. Mater.* 2016, **2,** 6306; d) J. Oh, K. Kranthiraja, C. Lee, K. Gunasekar, S. Kim, B. Ma, B. J. Kim, S.-H. Jin, *Adv. Mater.* 2016, **28**, 10016.

14. a) X. Long, Z. Ding, C. Dou, J. Liu, L. Wang, *Adv. Mater.* 2016, **28**, 6504; b) Y. Wang, Z. Yan, H. Guo, M. A. Uddin, S. Ling, X. Zhou, H. Su, J. Dai, H. Y. Woo, X. Guo, *Angew. Chem. Int. Ed.* 2017, **56**, 15304.

15. Y.-J. Hwang, B. A. E. Courtright, A. S. Ferreira, S. H. Tolbert, S. A. Jenekhe, *Adv. Mater.* 2015, **27**, 4578.

16. Y. Diao, Y. Zhou, T. Kurosawa, L. Shaw, C. Wang, S. Park, Y. Guo, J. A. Reinspach, K. Gu, X. Gu, B. Tee, C. Pang, H. Yan, D. Zhao, M. F. Toney, S. C. B. Mannsfeld, Z. Bao, *Nat. Commun.* 2015, **6**, 7955.

17. a) S. Liu, Z. Kan, S. Thomas, F. Cruciani, J.-L. Brdas, P. M. Beaujuge, *Angew. Chem. Int. Ed.* 2016, **55**, 12996; b) G. Ding, J. Yuan, F. Jin, Y. Zhang, L. Han, X. Ling, H. Zhao, W. Ma, *Nano. Energy* 2017, **36**, 356.

18. E. Zhou, J. Cong, Q. Wei, K. Tajima, C. Yang, K. Hashimoto, *Angew. Chem. Int. Ed.* 2011, **50**, 2799.

19. E. Zhou, J. Cong, K. Hashimoto, K. Tajima, *Adv. Mater.* 2013, **25**, 6991.

20. E. Zhou, M. Nakano, S. Izawa, J. Cong, I. Osaka, K. Takimiya, K. Tajima, *ACS Macro Lett.* 2014, **3**, 872.

21. M. Liu, J. Yang, C. Lang, Y. Zhang, E. Zhou, Z. Liu, F. Guo, L. Zhao, *Macromolecules* 2017, **50**, 7559.

22. J. Yang, F. Chen, B. Xiao, S. Sun, X. Sun, K. Tajima, A. Tang, E. Zhou, *Sol. RRL* 2018, **2**, 1700230.

23. a) Z.-G. Zhang, Y. Yang, J. Yao, L. Xue, S. Chen, X. Li, W. Morrison, C. Yang, Y. Li, *Angew. Chem. Int. Ed.* 2017, **56**, 13503; b) L. Gao, Z.-G. Zhang, L. Xue, J. Min, J. Zhang, Z. Wei, Y. Li, *Adv. Mater.* 2016, **28**, 1884.

24. B. Fan, L. Ying, P. Zhu, F. Pan, F. Liu, J. Chen, F. Huang, Y. Cao, *Adv. Mater.* 2017, **29**, 1703906.

25. Z. Li, X. Xu, W. Zhang, X. Meng, Z. Genene, W. Ma, W. Mammo, A. Yartsev, M. R. Andersson, R. A. J. Janssen, E. Wang, *Energy Environ. Sci.* 2017, **10**, 2212.

26. Y. Guo, Y. Li, O. Awartani, H. Han, J. Zhao, H. Ade, H. Yan, D. Zhao, *Adv. Mater.* 2017, **29**, 1700309.

27. L. Ye, X. Jiao, W. Zhao, S. Zhang, H. Yao, H. Ade, J. Hou, *Chem. Mater.* 2016, **28**, 6178.

28. H. Benten, T. Nishida, D. Mori, H. Xu, H. Ohkita, S. Ito, *Energy Environ.* Sci. 2016, **9**, 135.

29. G. Wang, N. D. Eastham, T. J. Aldrich, B. Ma, E. F. Manley, Z. Chen, L. X. Chen, M. O. d. I. Cruz, R. P. H. Chang, F. S. Melkonyan, A. Facchetti, T. J. Marks, *Adv. Energy Mater.* 2018, **8**, 1702173.

30. a) W. Su, Q. Fan, X. Guo, B. Guo, W. Li, Y. Zhang, M. Zhang, Y. Li, *J. Mater. Chem. A* 2016, **4**, 14752; b) W. Su, Q. Fan, X. Guo, X. Meng, Z. Bi, W. Ma, M. Zhang, Y. Li, *Nano Energy* 2017, **38**, 510.

31. a) Q. Fan, W. Su, X. Meng, X. Guo, W. Ma, M. Zhang, Y. Li, *Sol. RRL* 2017, **1**, 1700020; b) Q. Fan, W. Su, X. Guo, Y. Wang, J. Chen, C. Ye, M. Zhang, Y. Li, *J. Mater. Chem. A* 2017, **5**, 9204.

32. B. Xiao, A. Tang, J. Zhang, A. Mahmood, Z. Wei, E. Zhou, *Adv. Energy Mater.* 2017, **7**, 1602269.

33. B. Xiao, A. Tang, J. Yang, Z. Wei, E. Zhou, *ACS Macro Lett.* 2017, **6**, 410.

34. A. Tang, B. Xiao, Y. Wang, F. Gao, K. Tajima, H. Bin, Z. Zhang, Y. Li, Z. Wei, E. Zhou, *Adv. Funct. Mater.* 2018, **28**, 1704507.

35. Q. Fan, Z. Xu, X. Guo, X. Meng, W. Li, W. Su, X. Ou, W. Ma, M. Zhang, Y. Li, *Nano Energy* 2017, **40**, 20.

36. B. Guo, W. Li, X. Guo, X. Meng, W. Ma, M. Zhang, Y. Li, *Adv. Mater.* 2017, **29**, 1702291.

37. P. W. M. Blom, V. D. Mihailetchi, L. J. A. Koster, D. E. Markov, *Adv. Mater.* 2007, **19**, 1551.

38. P. Scherrer, *Kolloidchemie Ein Lehrbuch.* Springer Berlin Heidelberg: Berlin Heidelberg, 1912, 387-409.

39. J. Rivnay, M. F. Toney, Y. Zheng, I. V. Kauvar, Z. Chen, V. Wagner, A. Facchetti, A. Salleo, *Adv. Mater.* 2010, **22**, 4359.

40. a) X. Guo, N. Zhou, S. J. Lou, J. Smith, D. B. Tice, J. W. Hennek, R. P. Ortiz, J. T. L. Navarrete, S. Li, J. Strzalka, L. X. Chen, R. P. H. Chang, A. Facchetti, T. J. Marks, *Nat. Photonics* 2013, **7**, 825; b) G. J. Hedley, A. J. Ward, A. Alekseev, C. T. Howells, E. R. Martins, L. A. Serrano, G. Cooke, A. Ruseckas, I. D. W. Samue, *Nat. Commun.* 2013, **4**, 2867.

41. W. Ma, C. Yang, X. Gong, K. Lee, A. J. Heeger, *Adv. Funct. Mater.* 2005, **15**, 1617.

The table of contents entry

The efficient and thermally stable all-PSCs based on PFBZ:N2200 were developed and showed a high efficiency of 8.1%. After high temperature annealing at 150 ˚C for 180 min or ultrahigh temperature annealing at 250 ˚C for 15 min or storage at the N_2-filled glovebox for 1080 h, the all-PSCs still achieved the efficienies of more than 7%.

Keywords: Thermal stability; fluorinated wide bandgap polymer; power conversion efficiency; all-polymer solar cells

Efficient and thermally stable all-polymer solar cells based on a fluorinated wide bandgap polymer donor with high crystallinity

Wenyan Su, Yuan Meng, Xia Guo,* Qunping Fan, Zhuo Xu, Yu Dai, Beichen Xie, Maojie Zhang,* and Yongfang Li